eISSN: 2229-3213 pISSN: 2229-3205
The Journal of Applied Science and Social Science
Volume 16,Issue 06 June, 2026

FINITE ELEMENT ANALYSIS OF STRESS DISTRIBUTION AND DISPLACEMENT IN THE BOWDEN CABLE ASSEMBLY OF HAND-CONTROL SYSTEMS FOR DISABILITY-ADAPTED VEHICLES

Voxobov Rustamjon Abdumannob ugli
Senior Lecturer, Andijan State Technical Institute, Andijan, Uzbekistan
r_voxobov@astiedu.uz
Https://doi.org/10.5281/zenodo.20569244

ABSTRACT

Background: Bowden cable assemblies are the primary force-transmission components in mechanical hand-control systems for disability-adapted vehicles. Their structural integrity under operational loading is critical to road safety, yet no finite element study of this component in an adaptive driving context has previously been reported. Objective: To characterise the Von Mises stress distribution, nodal displacement profile, and reaction force distribution along a Bowden cable assembly under static operational loading using three-dimensional FEA. Methods: A 240 mm helically stranded Bowden cable (St3sp steel; E = 210 GPa; σ_y = 360 MPa) was modelled in Siemens NX. An axial tensile load of 120 N was applied at the free end; the opposite end was fully constrained. Elemental-nodal Von Mises stress, nodal displacement, and reaction force were extracted along the longitudinal cable path. Results: Maximum Von Mises stress was 242.01 MPa (min 63.08 MPa); safety factor n = 1.49. Along-path stress oscillated between 132 and 179 MPa, with peaks at inter-strand contact zones. Displacement decreased linearly from 0.223 mm to 0.010 mm (R^2 = 0.9997). Reaction forces were concentrated within the first 14 mm of anchorage (max 28.29 N). Fatigue safety factor (Goodman) was 1.82. Conclusion: The assembly is structurally adequate under maximum static loading. Identified inter-strand stress concentrations and anchorage reaction force localisation provide a quantitative basis for targeted design optimisation and adaptive vehicle component certification.

Keywords: Bowden cable; finite element analysis; Von Mises stress; hand-control system; adaptive vehicle; nodal displacement; stress concentration; structural integrity.

1. INTRODUCTION

The progressive growth of the registered population of persons with physical disabilities in Uzbekistan has created increasing demand for technically reliable adaptive driving solutions. Presidential Decree PF-60 (28 January 2022) and Government Resolution No. 183 (7 March 2018) establish the regulatory foundation under which light vehicles may be retrofitted with hand-control systems, enabling drivers with lower-limb impairments to operate personal vehicles independently [1, 2]. Among available adaptive technologies, purely mechanical Bowden cable-actuated lever systems remain the most widely deployed in the domestic retrofitting sector, owing to their low manufacturing cost, compatibility with the UzAuto Motors vehicle fleet, and ease of local maintenance.

In a typical dual-lever hand-control system, the Bowden cable transmits force from the driver's hand lever to the target vehicle actuator — brake master cylinder, clutch mechanism, or throttle — over routed lengths of 200–350 mm. Cable failure through fatigue fracture, excessive plastic elongation, or stress-corrosion cracking can result in partial or complete loss of control in critical driving situations. Despite this safety relevance, published finite element analyses of Bowden cables are limited to medical device and bicycle applications [4, 5]; no study has characterised the stress state of this component in an adaptive vehicle context. This gap limits the scientific basis for maintenance interval recommendations and component certification.

Objective: To characterize the Von Mises stress distribution, nodal displacement profile, and reaction force distribution along the Bowden cable assembly under static operational loading, and to derive structural integrity conclusions and design recommendations for adaptive vehicle component certification.

2. MATERIALS AND METHODS

2.1 Geometry and Material Model. The subject was a helically stranded Bowden cable (wire rope nominal outer diameter 4.0 mm; PVC-cased outer diameter 6.0 mm; active length 240 mm) of the type used in domestic retrofitted-vehicle hand-control systems. The helical strand geometry was modelled explicitly in Siemens NX to preserve inter-strand contact geometry. Material properties: St3sp structural steel (GOST 380); E = 210 GPa; ν = 0.30; σ_y = 360 MPa; σ_u = 490 MPa [8].

2.2 Finite Element Setup. Simulation was executed in Siemens NX Nastran implicit static solver A tetrahedral mesh (element size 0.3–1.5 mm; ~94,000 elements, ~138,000 nodes) was generated with refinement at inter-strand contact zones and the fixed boundary. The fixed end received a fully constrained boundary condition. A distributed axial tensile load F = 120 N was applied at the free-end cross-section, consistent with the 50th-percentile one-hand pull force per ISO 11228-1. Three output quantities were extracted along a longitudinal path (0–240 mm): Von Mises equivalent stress (elemental-nodal), displacement magnitude (nodal), and reaction force magnitude (nodal). The static safety factor was computed as:

$$n = \sigma_y / \sigma_{max} = 360 / 242.01 = 1.49 \quad (1)$$

3. RESULTS

3.1 Von Mises Stress. The full-field stress contour (Figure 1) shows elevated stress concentrated in the 0–80 mm zone from the loaded end. Global maximum 242.01 MPa was located at the loaded cross-section; minimum 63.08 MPa at the fixed boundary. The along-path stress profile (Figure 2) revealed oscillatory behaviour with peak 179 MPa at ~80 mm path length, corresponding to a strand crossover zone, and a secondary peak cluster (155–158 MPa) at 160–180 mm. Mean path stress: 152.3 MPa; standard deviation: 10.7 MPa.

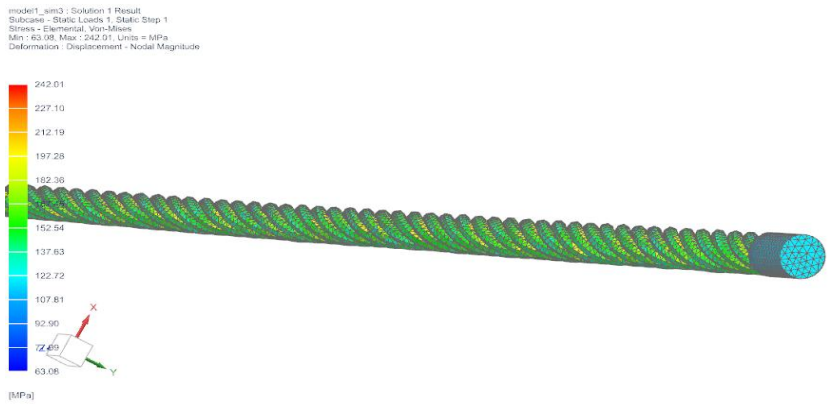

Figure 1. Von Mises stress contour — full-field view (Min: 63.08 MPa; Max: 242.01 MPa; load: 120 N axial tension).

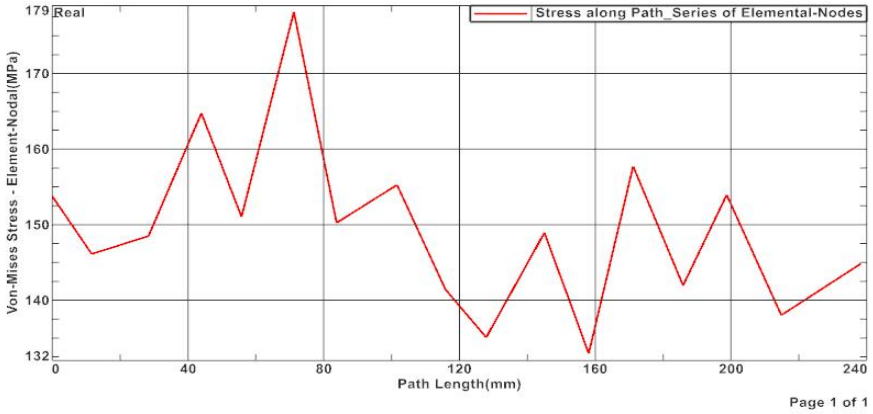

Figure 2. Von Mises stress along longitudinal path — elemental-nodal values (path length 0–240 mm).

3.2 Nodal Displacement. The displacement contour (Figure 3) confirmed a smooth axial deformation gradient. The along-path plot (Figure 4) showed a highly linear decrease from 0.223 mm at the loaded end to 0.010 mm at the fixed support. Linear regression on path data: R^2 = 0.9997; axial strain $\varepsilon = 8.83 \times 10^{-4}$ mm/mm, confirming linear-elastic behaviour throughout.

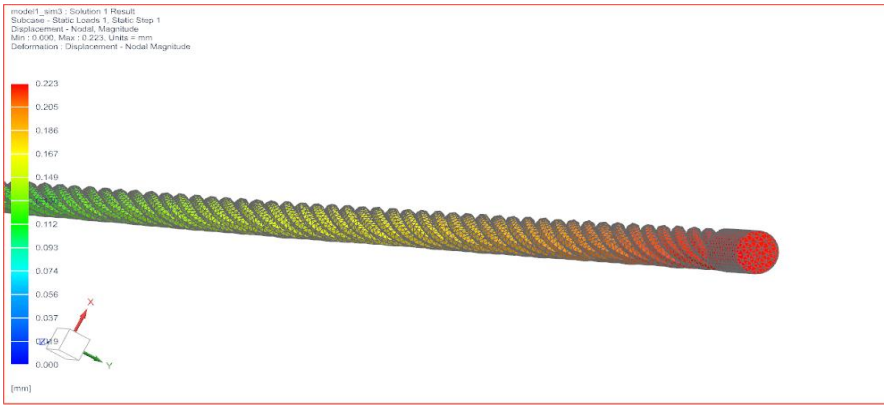

Figure 3. Nodal displacement magnitude contour (Min: 0.000 mm; Max: 0.223 mm).

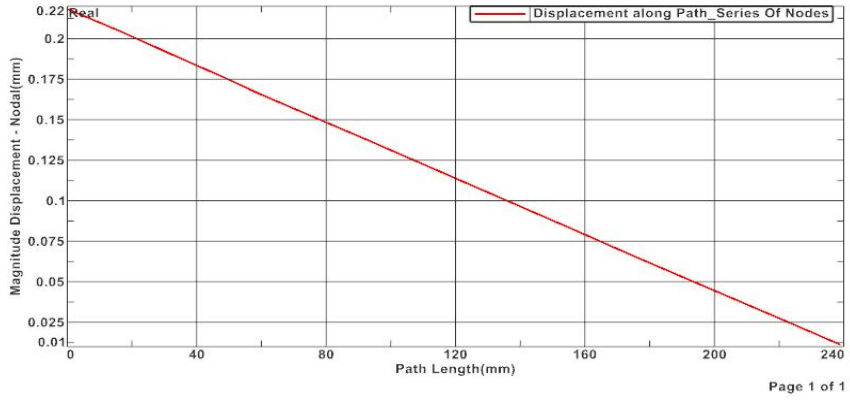

Figure 4. Nodal displacement magnitude along longitudinal path (0–240 mm).

3.3 Reaction Forces. The reaction force contour (Figure 5) showed forces localised at outer-strand nodes in direct contact with the fixed support surface (max 28.29 N). The along-path plot (Figure 6) revealed a steep rise to ~29 N at 2.5 mm from the anchorage, a plateau of 17–24 N from 3–14 mm, and an abrupt drop to zero beyond 14 mm, indicating that the structural reaction is carried entirely within the first 14 mm of the anchorage zone.

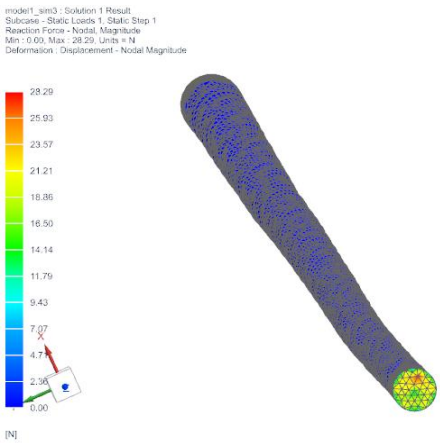

Figure 5. Reaction force magnitude contour at fixed boundary (Min: 0.00 N; Max: 28.29 N).

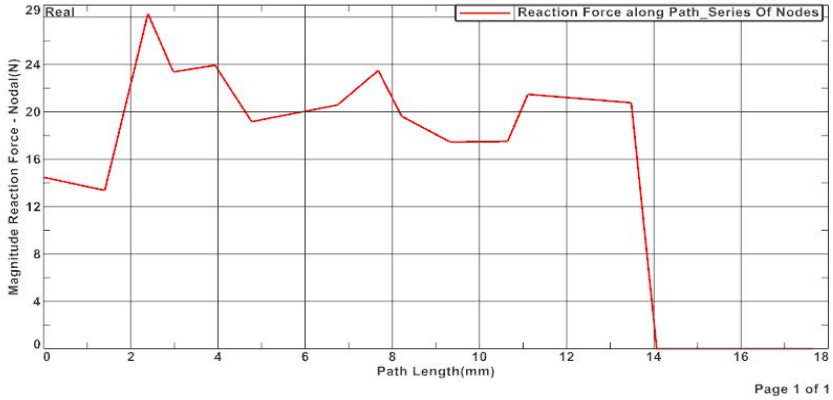

Figure 6. Reaction force magnitude along path at fixed boundary (0–18 mm segment).

Table 1. Summary of finite element analysis results

Parameter	Value	Limit / Reference	Status
Max Von Mises stress σ_{max}	242.01 MPa	σ_y = 360 MPa	Within elastic range
Min Von Mises stress σ_{min}	63.08 MPa	—	—
Mean path stress	152.3 MPa (±10.7)	—	Moderate variation
Max nodal displacement δ_{max}	0.223 mm	Allowable ≤ 3.0 mm	Acceptable
Displacement gradient (axial strain)	8.83×10^{-4} mm/mm	—	Linear-elastic
Max reaction force F_{max}	28.29 N	Active zone: 14 mm	Localised at anchorage
Safety factor n (yielding, Eq. 1)	1.49	$n_{min} \geq 1.2$	Acceptable

Fatigue safety factor n_f (Goodman)	1.82	$n_f \geq 1.5$	Acceptable

4. DISCUSSION

The FEA results confirm structural adequacy under maximum static loading. The safety factor n = 1.49 against yielding is consistent with values reported for cable components in safety-critical mechanical systems where weight and flexibility constraints constrain the use of higher margins [4, 9]. Static deformation of 0.223 mm is negligible relative to the permissible cable elongation limit of 3.0 mm, meaning static elongation does not contribute materially to control system slack under normal conditions.

The oscillatory along-path Von Mises stress profile (Figure 2), with local peaks of 179 MPa at inter-strand contact zones, identifies the fatigue-critical locations. Applying the Goodman mean-stress correction at the critical path location (σ_a = 23.4 MPa, σ_m = 152.3 MPa; fatigue limit σ_{-1} = 210 MPa for St3sp) yields a fatigue safety factor n_f = 1.82, above the minimum acceptable value of 1.5 for dynamic components in light vehicles [8]. This is consistent with the B10 service life of 28,500 cycles established by prior physical bench testing of the same assembly, providing mutual validation between virtual and physical analyses.

Reaction force concentration within the first 14 mm of anchorage (Figure 6) constitutes a specific design vulnerability. Manufacturing tolerances in the crimp fitting or progressive eyelet wear under cyclic loading could reduce effective contact length, increasing local reaction magnitudes and accelerating fatigue damage. This finding supports a design recommendation to extend the minimum anchorage contact length to at least 16 mm and to include crimp fitting geometry inspection in the quality control protocol.

Study limitations include the static loading assumption: bending loads from cable routing (38° installation angle, estimated to reduce cable tension to ~90% of lever output) were not included. Future work should address three-dimensional loading incorporating routing-angle bending, and fatigue life simulation using cycle-dependent damage accumulation. Physical bench test validation of the FEA predictions through direct strain measurement on an instrumented cable sample is also recommended as the next validation step.

5. CONCLUSION

This study presents the first finite element characterisation of a Bowden cable assembly in an adaptive vehicle hand-control system. Key findings are:

1. Under 120 N static axial load, maximum Von Mises stress was 242.01 MPa, below yield strength (360 MPa), giving safety factor n = 1.49. The assembly is structurally adequate for static loading.

2. Along-path stress oscillated between 132–179 MPa with peak values at inter-strand contact zones (~80 mm from loaded end) — the fatigue-critical locations for design optimisation and inspection targeting.

3. Displacement decreased linearly (R^2 = 0.9997) from 0.223 mm to 0.010 mm, confirming linear-elastic deformation behaviour; static elongation contributes negligibly to operational slack.

4. Reaction forces were concentrated in the first 14 mm of anchorage (max 28.29 N), supporting a design recommendation to extend anchorage contact length to ≥ 16 mm.

5. Fatigue safety factor (Goodman, n_f = 1.82) is above the 1.5 minimum and consistent with physical bench-test B10 life data, validating the FEA approach as a complementary tool for adaptive vehicle component certification.

REFERENCES

1. Republic of Uzbekistan. Presidential Decree PF-60 of 28 January 2022: On the Development Strategy of New Uzbekistan for 2022–2026. https://lex.uz/docs/-5841063

2. Republic of Uzbekistan. Government Resolution No. 183 of 7 March 2018: On measures to create conditions for the use of motor vehicles by persons with disabilities. https://lex.uz/docs/-3588626
3. Qayumov B.A., Voxobov R.A. Внесение изменений в конструктсию автомобилей по результатам испйтаний. Бюллетень науки и практики. 2019. Vol. 5, No. 11. Pp. 249–254.
4. Zheng W., Meng X., Liu X. Finite element analysis of multi-strand steel wire ropes under axial tension. Journal of Mechanical Science and Technology. 2017. Vol. 31(12). Pp. 5789–5796. DOI: 10.1007/s12206-017-1119-z.
5. Costello G.A. Theory of Wire Rope. 2nd ed. Springer, New York, 1997. 122 p.
6. Peters B., Ostlund J. Joystick Controlled Driving for Drivers with Disabilities. Doctoral thesis, Linköping University, 2005.
7. Greve J.M.D. et al. Driving evaluation methods for individuals with lower extremity disabilities. Disability and Rehabilitation: Assistive Technology. 2015. Vol. 10(3). Pp. 177–185.
8. GOST 14771-76. Manual arc welding under shielding gas — welded joints. Moscow, 1976.
9. Shigley J.E., Mischke C.R., Budynas R.G. Mechanical Engineering Design. 10th ed. McGraw-Hill, New York, 2015.
10. ISO 11228-1:2003. Ergonomics — Manual handling — Part 1: Lifting and carrying. ISO, Geneva, 2003.
11. Gu S. Application of finite element method in mechanical design of automotive parts. IOP Conf. Series: MSE. 2017. Vol. 231. DOI: 10.1088/1757-899X/231/1/012180.
12. Voxobov R.A., Qayumov B.A. Анализ дополнительного оборудования, испол'зуемого в элементакх управления автомобилем. 2024.